JOURNAL OF GEOPHYSICAL RESEARCH, VOL. 108, NO. B3, 2158, doi:10.1029/2001JB000550, 2003

Implications of the shear stress river incision model for the timescale of postorogenic decay of topography

Julia A. Baldwin and Kelin X. Whipple

Department of Earth, Atmospheric, and Planetary Sciences, Massachusetts Institute of Technology, Cambridge, Massachusetts, USA

Gregory E. Tucker

School of Geography and the Environment, University of Oxford, Oxford, UK

Received 30 March 2001; revised 18 June 2002; accepted 22 October 2002; published 18 March 2003.

[1] The reason for the survival of mountainous topography in ancient orogenic belts is a long-standing problem in geomorphology and geodynamics. We explore the geomorphologic controls on the timescale for the postorogenic decay of topography to address the question of whether there is a viable geomorphologic explanation for the persistence of topography in ancient orogenic belts or whether alternative geodynamic explanations must be sought. Using both approximate analytical solutions and numerical simulations, we show that the standard detachment-limited stream power river incision model predicts, for reasonable initial topographies, relatively short postorogenic decay times of 1–10 Myr. Additional layers of complexity are introduced to this simplest model including isostasy and flexural strength, a transition to transport-limited conditions during decline, and the incorporation of the combined effects of a critical threshold for erosion and the stochastic variability of flood magnitudes. Each of these additional factors acts to lengthen the decay timescale. Pure Airy isostatic rebound of a thick crustal root results in decay times that are at most a factor of 6 longer than the detachment-limited result. The transition to transport-limited conditions involves partial protection of the bed by a thin layer of alluvium, which inhibits erosion and therefore increases decay times by a factor of 2–3 in our analysis. Finally, including critical shear stress results increases decay time by approximately a factor of 20 for the parameter values in our example calculation. More importantly, however, a significant portion of topography remains after predicted lowering rates have dropped to values less than measured rates of denudation in weathering-limited, low-relief environments. Thus a model combining isostasy, a transition to transport-limited conditions, and a critical shear stress for erosion could account for the presence of residual topography for hundreds of million years. All three of these factors can be expected to play a role in natural settings. *INDEX TERMS:* 1815 Hydrology: Erosion and sedimentation; 1824 Hydrology: Geomorphology (1625); 8110 Tectonophysics: Continental tectonics—general (0905); *KEYWORDS:* topography, erosion, relief, postorogenic, geomorphology

Citation: Baldwin, J. A., K. X. Whipple, and G. E. Tucker, Implications of the shear stress river incision model for the timescale of postorogenic decay of topography, *J. Geophys. Res.*, *108*(B3), 2158, doi:10.1029/2001JB000550, 2003.

1. Motivation

[2] The persistence of mountainous topography in ancient orogenic belts is a long-standing unsolved problem. A surprisingly large number of Paleozoic orogenic belts retain a subdued, but distinctly mountainous morphological expression (e.g., Appalachians, Caledonides, Canadian Rockies, Lachlan fold belt of southeastern Australia, Ural Mountains, and several Paleozoic ranges in central Asia). Geomorphologists have pondered the timescale of postorogenic topographic decay for over a century, at least since the original statement of William Morris Davis' theory of landscape evolution [*Davis*, 1889]. Much debate centered on the question of the time required for the development of peneplains [*Davis*, 1925; *Gilluly*, 1955; *Schumm*, 1963; *Judson and Ritter*, 1964; *Melhorn and Edgar*, 1975; *Twidale*, 1976; *Fairbridge and Finkl*, 1980; *Pazzaglia and Brandon*, 1996]. *Stephenson* [1984] argued that the persistence of topography might simply reflect isostatic compensation of crustal roots, while others [e.g., *Hack*, 1982; *Pazzaglia and Gardner*, 1994] have suggested postorogenic uplift processes, possibly related to mantle dynamics.

0148-0227/03/2001JB000550$09.00

[3] Early quantitative analyses estimated decay times by dividing mean elevation by average denudation rates. Most of these analyses yielded estimates of 10–25 Myr to reduce mountainous topography to baselevel [*Gilluly*, 1955; *Schumm*, 1963; *Judson and Ritter*, 1964]. For the continental United States, *Gilluly* [1955] estimated 10 Myr with spatially averaged erosion and no isostatic compensation, and 33 Myr with erosion concentrated in mountainous areas and accounting for isostatic compensation of crustal roots. Later analyses exploited data suggesting a correlation between denudation rate and elevation (implying an exponential decline in mean elevation with time) to estimate a decay timescale that is effectively a topographic half-life [*Pinet and Souriau*, 1988; *Pazzaglia and Brandon*, 1996]. In the most recent treatment of this type, *Pazzaglia and Brandon* [1996] find a global average decay timescale (which they argue is applicable to the present-day Appalachians) of 69 Myr, including the effects of isostatic compensation.

[4] Although some authors have argued that decay timescales must be much longer, at least in arid regions [*Twidale*, 1976; *Fairbridge and Finkl*, 1980], these analyses all leave room for the formation of multiple-peneplanation surfaces in ancient orogenic belts [e.g., *Melhorn and Edgar*, 1975], and suggest that postorogenic uplift events are needed to explain the survival of mountainous topography in Paleozoic orogenic belts [e.g., *Pazzaglia and Brandon*, 1996].

[5] Relief and landscape response timescale depend primarily on bedrock channels [e.g., *Whipple and Tucker*, 1999; *Whipple*, 2001], plus a lag time associated with hillslope response [e.g., *Fernandes and Dietrich*, 1997]. Therefore in order to examine the postorogenic decay of topography from a geomorphologic perspective, it is necessary that we first understand the controls on river incision into bedrock. Most recent research has focused on bedrock channel erosion processes and their role in landscape evolution [*Seidl and Dietrich*, 1992; *Howard*, 1994; *Wohl et al.*, 1994; *Sklar and Dietrich*, 1998; *Slingerland et al.*, 1998; *Tinkler and Wohl*, 1998; *Slingerland*, 1999; *Whipple and Tucker*, 1999; *Whipple*, 2001]. Partly driven by interest in the dynamic coupling between tectonics and climate, most research on bedrock channels has emphasized active tectonic settings [e.g., *Hancock et al.*, 1998; *Pazzaglia et al.*, 1998; *Sklar and Dietrich*, 1998; *Wohl*, 1998; *Snyder et al.*, 2000]. Postorogenic landform evolution has not received much attention in the past decade of intense research on bedrock channels despite the widespread occurrence and importance of postorogenic landforms and processes.

[6] In addition to isostatic uplift of a crustal root and postorogenic uplift driven by evolving mantle dynamics, a number of plausible geomorphologic explanations for the persistence of topography can be entertained. In the simplest terms, a geomorphologic explanation requires that postorogenic erosion is very slow, implying a progressive decline in erosion rates through time as topography is reduced. In fact, there is evidence, based on suspended sediment loads, that old orogens have lower effective erosion rates than young orogens [*Pinet and Souriau*, 1988]. Different formulations of the river incision problem can be expected to predict differing degrees to which erosion rates decline over time. In addition, various river incision models predict differing characteristic forms of residual topography, which provide an important additional constraint on the range of viable river incision models [*Tucker and Whipple*, 2002]. In order to address the various possibilities, we ask the question: what are the important geomorphic controls on the timescale of postorogenic topographic decay? We find that these controls include synorogenic uplift rate, lithology, climate, channel bed alluviation during topographic decline, flexural isostatic response, and the magnitude of a critical shear stress for channel bed erosion. We assess the relative importance of these controls and the extent to which geomorphic processes provide a viable explanation for the persistence of mountainous topography in ancient orogens.

2. Characteristics of Ancient Mountain Belts

[7] Of the many Paleozoic orogenic belts still marked by mountainous topography, only a few have been sufficiently well studied to provide a motivational framework for our analysis of the controls on topographic decay timescale. The southern Appalachians, the Lachlan fold belt of southeastern Australia, and the Ural Mountains are the prime examples. The geomorphology and long-term evolution of the first two of these have been extensively studied. Considerable work on the geomorphology of the Ural Mountains is published primarily in Russian. Subsequently, we briefly summarize the key characteristics of each orogenic belt that importantly constrain and guide our analysis. As our analysis considers only nonglacial erosion processes, the Canadian Rockies, the Caledonides, and northern Appalachians must be excluded.

2.1. Topography and Channel Longitudinal Profiles

[8] Each of these Paleozoic orogenic belts is marked by subdued but mountainous topography. Hillslope gradients in excess of the angle of repose are common in areas of resistant lithology. Peak elevations in excess of 1500 m are not uncommon, and mean elevation rises some 1000 m above the surrounding terrain in all cases. Studies by *Hack* [1957, 1975] in the Appalachians and by Bishop et al. in the Lachlan fold belt [*Bishop et al.*, 1985; *Goldrick and Bishop*, 1995; *Bishop and Goldrick*, 2000; *Young*, 1989; *Young and McDougall*, 1993] have clearly documented that channel longitudinal profiles are consistent with an approximate "dynamic equilibrium" between river incision and isostatic uplift in the short term, even though relief may be gradually declining over the long term [i.e., see discussion of timescales by *Schumm and Lichty*, 1965]. In both ranges, where not disturbed by contrasts in lithology [*Hack*, 1957, 1975, 1982; *Bishop et al.*, 1985; *Goldrick and Bishop*, 1995; *Bishop and Goldrick*, 2000], channel profiles show semilogarithmic forms (smooth, concave-up profiles) that are very similar to "steady state" forms expected and observed in actively uplifted ranges [e.g., *Whipple and Tucker*, 1999; *Snyder et al.*, 2000]. In addition, in both ranges, channels have mixed alluvial-bedrock bed morphologies with stream gradient locally adjusted to the size of the bed load [*Hack*, 1957; *Bishop et al.*, 1985] suggesting transport-limited conditions. Our own analyses (K. X. Whipple, unpublished data) have confirmed that similar channel profile forms

dominate the Blue Ridge and Valley and Ridge provinces in the Appalachians (including many channels not included in Hack's analysis) and are characteristic of the southern Ural Mountains (topographic data available only south of 54°N latitude).

2.2. Antiquity and Postorogenic Evolution

[9] The Ural Mountains have received comparatively little attention in the English literature, but there has been considerable debate about the postorogenic evolution of both the Appalachians and the Lachlan fold belt. Both belts experienced their last phase of compressional orogenesis in the Paleozoic (Permian and Late Devonian-Early Carboniferous, respectively) [*Judson*, 1975; *Gray*, 1997]. However, both were overprinted by Mesozoic rifting with commensurate thermal and flexural uplift [*Judson*, 1975; *Gray*, 1997]. Major postorogenic drainage reorganizations are debated for both ranges [e.g., *Davis*, 1889; *Thornbury*, 1962; *Meyerhoff*, 1972; *Judson*, 1975]. Thus both ranges have experienced complex histories, and the antiquity of the topography is uncertain. However, even a Mesozoic age for the development of initial topography is problematic given the short (~10–25 Myr) topographic decay times predicted by most previous analyses [*Gilluly*, 1955; *Schumm*, 1963; *Judson and Ritter*, 1964]. Traditional interpretations in both the Appalachians and the Lachlan fold belt have called for accelerated Late Cenozoic uplift [Lachlan: e.g., *Wellman*, 1979; *Ollier*, 1978, 1982, 1985; *Ollier and Pain*, 1994, 1996; *Stephenson and Lambeck*, 1985; *Lister and Etheridge*, 1989; *Brown et al.*, 1994; *Browne*, 1969; Appalachians: e.g., *Judson*, 1975; *Melhorn and Edgar*, 1975; *Pazzaglia and Brandon*, 1996; *Poag et al.*, 1989].

[10] Although it is possible that Late Cenozoic "epiorogenic" uplift has occurred in some ancient orogenic belts [e.g., *Pazzaglia and Brandon*, 1996], recent studies in the Lachlan fold belt strongly suggest that in the modern topography there is in fact a remnant of a Paleozoic mountain range. *Lambeck and Stephenson* [1985] demonstrated with a simple elevation-dependent erosion model that both modern topography and evidence for Plio-Pleistocene uplift and river incision are consistent with isostatic compensation of slow, continuous erosion since the Paleozoic. Young and colleagues [*Bishop et al.*, 1985; *Bishop and Goldrick*, 2000; *Young*, 1989; *Young and McDougall*, 1993] have presented fairly convincing evidence that: (1) the modern drainage divide follows the axis of a pronounced gravity low for 80% of its 3800 km length; (2) the modern drainage pattern was in place by 20 Ma and has evolved little since; and (3) there is little difference between modern stream channels (gradient, sediment size) and their Miocene progenitors. Finally, *van der Beek and Braun* [1999] concluded from their modeling study that a significant percentage of the paleo-topography dated to the Paleozoic (prerift).

2.3. Gravity and Isostasy

[11] Excess crustal roots appear to be characteristic of ancient orogenic belts. Each of the Appalachians, Lachlan fold belt, and the Ural Mountains is marked by a well-defined negative gravity anomaly on the order of 40–50 mGals [*Jacobs et al.*, 1959; *Young*, 1989; *Wellman*, 1979; *Berzin et al.*, 1996]. Seismic data corroborates an interpretation that this represents excess crustal thickness on the order of 45–50 km [e.g., *Young*, 1989; *Costain et al.*, 1989]. Such large crustal roots are in excess of that needed to isostatically compensate the residual topography. Therefore models assuming full isostatic compensation probably overestimate the topographic decay timescale.

[12] In the case of the Urals, the interpretation of available geophysical data is unclear with regard to the question of how isostatic compensation of a crustal root has influenced the preservation of mountainous topography since the Paleozoic. Here maximum crustal thicknesses of 55–58 km indicate the presence of a 12–15 km thick crustal root. However, the topographic axis of the Urals is offset from the crustal root by ~100–150 km, which suggests that present topography is unrelated to crustal thickness and represents remnant relief from Paleozoic deformation [*Berzin et al.*, 1996; *Carbonell et al.*, 1996]. It has been proposed that a dense crustal or mantle lithosphere load is in part responsible for the root, and that this apparent subcrustal load is in fact mantle material beneath a thinned crust [*Kruse and McNutt*, 1988].

Table 1. List of Models Used in This Analysis

Models Used	Type
1	detachment-limited
2	detachment-limited with isostatic rebound
3	transition to transport-limited conditions during decline
4	stochastic distribution of floods and critical shear stress

3. Approach and Scope

[13] This paper is a general, theoretical exploration of the geomorphic controls on the timescale of postorogenic topographic decay. The analysis is intentionally restricted to fluvial erosion processes and the fluvial component of landscape relief. Thus any lag time associated with hillslope response [e.g., *Fernandes and Dietrich*, 1997] is not considered. We examine first a standard formulation of the detachment-limited stream power river incision model (Model 1), and then consider in turn additional layers of complexity, including isostatic rebound (Model 2), a transition to transport-limited conditions during topographic decline (Model 3), and the combined effects of a stochastic distribution of flood discharges and a critical shear stress for erosion (Model 4) (Table 1) [e.g., *Tucker and Bras*, 2000]. In all model runs we hold climate, drainage pattern, and base level constant, recognizing that this is a simplified, theoretical treatment. Ancient orogens with remnant topography have undoubtedly experienced long and complicated histories, and in such orogenic belts as the Appalachians this simplified scenario does not directly apply. Therefore this study is not intended to be a quantitative analysis of the protracted history of topography and exhumation in any specific orogenic belt. Our aim instead is to evaluate the most general controls and geomorphic constraints on postorogenic decay time.

[14] *Whipple* [2001] recently extended and generalized the approximate analytical solution for fluvial response time to a change in uplift rate for the stream power

detachment-limited river incision model given by *Whipple and Tucker* [1999]. In order to examine the postorogenic evolution of topography, we modify the *Whipple* [2001] response time solution for the case of a sudden (step-function) cessation of rock uplift. One of the main goals of this analysis is to examine how the decay time is affected by the various parameters of the shear stress law, including the synorogenic uplift rate, the length of the channel, and the erodibility of the channel, which incorporates many different factors such as lithology, rock strength, channel bed material, sediment flux, channel width, and annual precipitation [e.g., *Howard et al.*, 1994; *Sklar and Dietrich*, 1998; *Whipple and Tucker*, 1999; *Whipple et al.*, 2000; *Snyder et al.*, 2000]. As discussed by *Weissel and Seidl* [1998], *Whipple* [2001], and *Royden et al.* [2000], for the declining case (decrease in uplift rate), the approximate analytical solution given by *Whipple and Tucker* [1999] can be expected to significantly underestimate response time if incision rate is dependent on channel gradient to a power greater than unity. In this case, steeper parts of the migrating break in slope move faster upstream (This ''slope break'' is referred to as a ''knickpoint'' in the work of *Whipple and Tucker* [1999] and *Whipple* [2001].) For the declining case this means the slope break loses definition, changes in channel gradient occur upstream of the otherwise expected position of the slope break, and there is a progressive reduction in erosion rate at the channel head. This declining rate of relief reduction naturally leads to longer response times. We use one-dimensional numerical simulations to illustrate this effect and to explore the consequences of a detachment-limited incision model. We next consider the impact of flexural isostatic compensation on predicted topographic decay timescales. Subsequently, we explore the consequences of an expected transition from detachment- to transport-limited conditions during topographic decline [*Whipple and Tucker*, 2002]. Finally, we explore briefly the role of a critical shear stress for channel bed erosion. For reasons that will become apparent, the consequences of including a critical shear stress cannot be adequately discussed without incorporating some representation of the stochastic variation of flood magnitudes. We employ the stochastic-storm-driven detachment-limited model used by *Tucker and Bras* [2000] in this analysis. The potentially important role of decreasing orographic precipitation as topography is reduced by erosion is not considered, but it can be inferred that this will somewhat increase predicted decay times.

4. Detachment-Limited Stream Power River Incision Model

4.1. Theoretical Background

[15] Incision of rivers into bedrock under detachment-limited conditions is often described by the shear stress (or stream power) model [e.g., *Howard and Kerby*, 1983; *Howard*, 1994; *Howard et al.*, 1994; *Rosenbloom and Anderson*, 1994; *Moglen and Bras*, 1995; *Tucker and Slingerland*, 1996; *Stock and Montgomery*, 1999; *Snyder et al.*, 2000; *Whipple et al.*, 2000; *Seidl and Dietrich*, 1992]. River incision described by the shear stress model results in a channel profile evolution equation, which can be written in two alternative forms:

$$\frac{dz}{dt} = U - K'(\tau_b - \tau_c)^a, \tag{1a}$$

$$\frac{dz}{dt} = U - K'\left(\tau_b^a - \tau_c^a\right), \tag{1b}$$

where dz/dt is the rate of change of channel bed elevation, U is the rock uplift rate relative to baselevel, K' is a dimensional coefficient of erosion [L^{1-2m}/T^1] reflecting both rock mass quality and erosion process, τ_b is the basal shear stress, and τ_c is a critical shear stress for detachment of bedrock blocks. Although equation (1a) is the usual form, there are no presently available empirical or theoretical grounds for discarding the more tractable form of equation (1b). Using the power function relationship between basal shear stress τ_b and drainage area A and slope S ($\tau_b = k_b A^{m'} S^{n'}$ where k_b is an erosion coefficient), equation (1) can be written in a more familiar form:

$$\frac{dz}{dt} = U - K\left(A^{m'}S^{n'} - \frac{\tau_c}{k_b}\right)^a, \tag{2a}$$

$$\frac{dz}{dt} = U - KA^mS^n + K'\tau_c^a, \tag{2b}$$

where $K = K'k_b{}^a$, $m' = m/a$, and $n' = n/a$ and a, m, and n are positive constants that reflect the mechanics of the erosion process, basin hydrology, and channel geometry [e.g., *Howard et al.*, 1994; *Hancock et al.*, 1998; *Whipple and Tucker*, 1999]. The threshold shear stress term is often neglected in analyses of bedrock channel evolution. Dropping the critical shear stress reduces either form of equation (2) to the familiar relation with incision rate E given as a power law function of drainage area and channel gradient ($E = KA^mS^n$) Dropping the τ_c term is effectively equivalent to making the assumption that the floods of interest in bedrock channel incision greatly exceed this threshold. We start with this assumption, in keeping with standard formulation of the stream power law, and return to the implications of omitting this term in a later section. Figure 1 shows schematically the response of the bedrock channel system to a decrease in uplift rate that is similar to the uplifting case [*Whipple and Tucker*, 1999; *Tucker and Whipple*, 2002].

[16] Longitudinal profiles of bedrock streams are often observed to follow a power law relationship between channel gradient and drainage area [e.g., *Flint*, 1974; *Tarboton et al.*, 1989]:

$$S = k_s A^{-\theta} = k_s k_a^{-\theta} x^{-h\theta}, \tag{3}$$

where θ is the concavity index of the channel, k_s is the steepness index, and k_a and h describe the relation between downstream position and upstream drainage area (h is the inverse of the Hack exponent) [*Hack*, 1957]. For $h\theta = 1$ (typical estimates of $h\theta$ are $0.6 \leq h\theta \leq 1.1$), equation (3) predicts a semilogarithmic channel form consistent with observations in several ancient orogens [*Hack*, 1957, 1975,

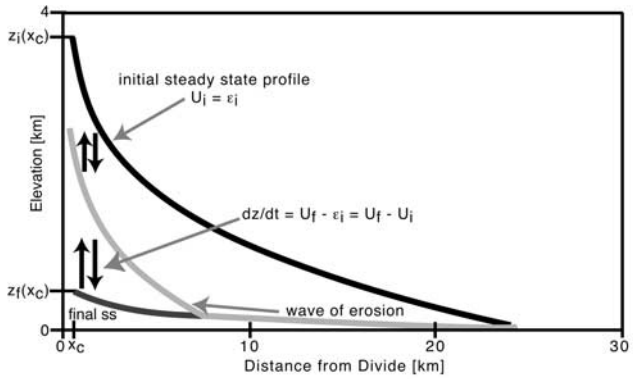

Figure 1. Schematic diagram of bedrock channel response to a decrease in uplift rate. A "decaying" transient is shown that might follow either a decrease in uplift rate or an increase in coefficient of erosion. A migrating break in slope separates an upstream segment that has not declined from a downstream segment that has responded to the new uplift rate. The gradient at the channel head remains unchanged until this slope break has swept through the entire system, so that the rate of channel head elevation change is constant as indicated for either tectonic or climatic perturbations [modified from the work of *Whipple and Tucker*, 1999].

1982; *Bishop et al.*, 1985; *Goldrick and Bishop*, 1995; *Bishop and Goldrick*, 2000]. This slope-area relationship is valid for detachment-limited systems only at steady state, but applies throughout decline if the system is transport-limited as channel profiles maintain a "characteristic form" given by a constant value of θ in equation (3) [*Willgoose*, 1994] (Figure 1). Under steady state conditions ($dz/dt = 0$) with uniform U and K, constant m and n, and negligible τ_c, the relationship between channel gradient and drainage area (from equation (2)) is given as:

$$S_d = \left(\frac{U}{K}\right)^{1/n} A^{-\theta_d}, \tag{4a}$$

$$\theta_d = m/n, \tag{4b}$$

where θ_d is termed the *intrinsic* concavity index of detachment-limited systems. Equation (4) predicts a power law relationship between channel gradient and drainage area which is observed in natural landscapes in the form of equation (3) [e.g., *Tarboton et al.*, 1991; *Sklar and Dietrich*, 1998], where the coefficient $(U/K)^{1/n}$ sets the channel steepness k_s. Following the work of *Whipple and Tucker* [1999, 2002] and *Kirby and Whipple* [2001], we refer to the ratio m/n (θ_d) as the intrinsic channel concavity index, which equals the actual concavity θ only at steady state under conditions of uniform U, K, m, and n. For shear stress driven fluvial erosion processes, *Whipple and Tucker* [1999] showed that for a pure detachment-limited system the intrinsic concavity index depends only on the relative rate of increase of: (1) channel width with discharge, and (2) discharge with drainage area. Typical estimates of the concavity index for channel profiles in tectonically active fluvial landscapes are consistent with theoretical predictions that the m/n ratio should fall within a narrow range near 0.5 ($0.35 \leq m/n \leq 0.6$) for fluvial erosion processes [*Tarboton et al.*, 1989; *Whipple and Tucker*, 1999; *Snyder et al.*, 2000; *Kirby and Whipple*, 2001]. Given this observation, the m/n ratio is held constant at 0.45 for all analyses herein. The slope exponent n, on the other hand, is not well constrained, importantly influences fluvial response time [*Whipple and Tucker*, 1999; *Whipple*, 2001], and may vary with the dominant erosion process (which may depend on substrate lithology) [e.g., *Hancock et al.*, 1998; *Whipple et al.*, 2000]. Theoretical predictions of the value of n range from $\sim$2/3 for soft, erodible material [*Howard and Kerby*, 1983], to $\sim$5/3 for erosion due to impact abrasion [*Foley*, 1980; *Hancock et al.*, 1998; *Whipple et al.*, 2000]. To explore its influence on topographic decay time, we vary n from 2/3 to 2.

4.2. Approximate Analytical Solution and Implications

[17] *Whipple* [2001] (equation (6)) gives a generalized form of the response time estimate first published by *Whipple and Tucker* [1999]:

$$T_D = \beta K^{-1/n} U_i^{1/n-1} \left(f_U^{1/n} - 1\right)(f_U - 1)^{-1}; \qquad f_U \neq 1, \tag{5}$$

where $f_u = U_f/U_i$ (the fractional change in rock uplift rate) and β is an entirely geometric term which depends on basin size, shape, and drainage density [*Whipple*, 2001] (equations (2a)–(2b):

$$\beta = k_a^{-m/n} \left(1 - \frac{hm}{n}\right)^{-1} \left(L^{1-hm/n} - x_c^{1-hm/n}\right); \qquad \frac{hm}{n} \neq 1. \tag{6}$$

[18] For the case of a sudden cessation of rock uplift, $U_f = 0$ and equation (5) reduces to:

$$T_D = \beta K^{-1/n} U_i^{1/n-1}. \tag{7}$$

[19] Derivation of equations (5)–(7) exploits the observation that the channel head gradient (at $x = x_c$) does not change until the migratory knickpoint (or slope break) reaches the channel head as illustrated in Figure 1 [*Whipple and Tucker*, 1999; *Whipple*, 2001]. Therefore the lowering rate at $x = x_c$ remains constant at the initial steady state erosion rate throughout the transient adjustment. This formulation breaks down for $n > 1$ because the migrating knickpoint loses definition and the gradient at the channel head (and therefore the lowering rate) begins to decline by the time relief has been reduced to $\sim$50% of the original relief. The interesting behavior of the $n > 1$ case results from the dependence of wave celerity (C_e) on channel gradient ($C_e \sim S^{n-1}$) [*Whipple and Tucker*, 1999; *Whipple*, 2001]. For $n > 1$ steeper portions of a migrating waveform (the knickpoint) propagate faster. As a result, the migrating knickpoint is rapidly dissipated and channel gradients decline rapidly upstream of the expected position of the knickpoint [*Sinclair and Ball*, 1996; *Weissel and Seidl*, 1998; *Royden et al.*, 2000; *Tucker and Whipple*, 2002]. This causes a progressive decline in erosion rate of the channel head and thus a marked increase in topographic

Table 2. Representative Decay Times (Time to Reduce to 1% of Original Topography at the Channel Head) for Approximate Analytical Solution for Initial Uplift Rate of 1 mm/yr

L, km	$z_i(x_c)$, m	T_D, years
10	1980[a]	1.96×10^6
50	3670[a]	3.63×10^6
100	4630[a]	4.58×10^6

[a]Elevation calculated from steady state channel profile, holding $(U/K)^{1/n}$ constant for $n = 2/3$, 1, and 2. For $n = 2/3$, $K = 2.92 \times 10^{-5}$; $n = 1$, $K = 5 \times 10^{-6}$; $n = 2$, $K = 2.5 \times 10^{-8}$.

decay time (Table 2). Therefore for $n > 1$ equation (5) can be expected to significantly underestimate topographic decay time [see additional discussion in the study of *Whipple*, 2001], so we use numerical simulations to evaluate this case.

[20] From equation (5), it can be seen that the decay timescale exhibits a power law dependence on the initial steady state uplift rate, with a power equal to $1/n - 1$. This relationship reflects a dual dependence on the initial uplift rate. Whereas steady state fluvial relief scales with $U^{1/n}$ (equation (4)), the erosion rate at the channel head scales linearly with U (T_D = initial relief/erosion rate $\sim U^{(1/n)-1}$). Thus decay time increases with initial uplift rate for $n > 1$ and is independent of the initial uplift rate for $n = 1$ (Figure 2a). Therefore for $n = 1$ no matter what the uplift rate is prior to erosion, the decay time is the same for any steady state profile for a given K and L. Numerical simulations are used below to examine the $n > 1$ case. Equation (5) further shows that decay timescale decreases as K increases ($T_D \sim K^{-1/n}$) for all values of n (Figure 2b). For large drainage basins ($L \gg x_c$) decay timescales with L to the $1 - hm/n$ power (Figure 2c). The exponent ($1 - hm/n$) typically varies from -0.10 to 0.40 and is held constant at 0.25 herein. Thus the decay timescale exhibits a relatively weak dependence on basin size.

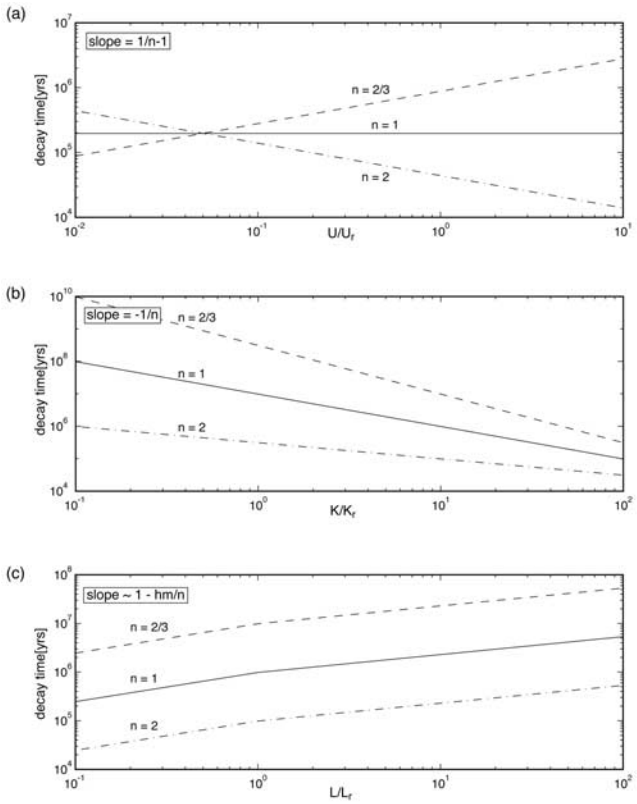

Figure 2. Relative dependence of decay timescale on U, K, and L for different values of n. Plots are in log-log space and U, K, and L are plotted against a single-reference value. Slopes of lines give the scaling exponents shown in outlined box.

[21] In order to define the "decay time" for both analytical and numerical solutions, it is necessary to specify criteria for attainment of "final" topographic decay. Two natural choices are to terminate simulations either when dz/dt declines to some threshold value (e.g., 0.001 mm/yr), or when channel head elevation ($z(x_c)$) declines to some threshold percentage of the original topography (e.g., 1%). In analytical solutions, the decay times were calculated for a threshold percentage of 1% of the original relief. In all numerical runs, the decay time was chosen where either topography reached 1% of the original relief or where erosion rates reached 0.001 mm/yr, whichever came first. Weathering likely becomes the dominant process once erosion rates are reduced to <0.005 mm/yr [*Bierman and Turner*, 1995; *Heimsath et al.*, 1997; *Small et al.*, 1997, 1999], so by running models out to erosion rates of 0.001 mm/yr, it seems reasonable to expect that beyond this time fluvial erosion is no longer setting lowering rates. However, this difference in criteria can become important in models that involve an asymptotic decay of topography to some final state (as in the case for $n > 1$). In some instances, it is also useful to compare decay time to the remaining percent of relief (50, 25, 10%, etc.).

[22] Representative decay times for the approximate analytical solution are given in Table 3. Typical decay times for reasonable initial channel head elevations (2000–4000 m) produced from an initial uplift rate of 1 mm/yr and channel lengths between 10 and 100 km range from ~2 to 5 Myr (for $n \leq 1$). In Table 4, K was varied to produce the same magnitudes of initial topography for different values of n. Holding $(U/K)^{1/n}$ constant results in decay times that are invariant with n. While arbitrarily low values of K (very resistant rocks and/or low discharge) will predict very long timescales, they would predict unrealistic initial topographies (e.g., $n = 1$, $K = 1 \times 10^{-8}$ predicts an initial topography of 9.9×10^5 m and a decay time of 840 Myr). This is why we argued in the introduction that the long persistence of mountainous topography requires a progressive decline in erosional efficiency with time. In section 5, we show that for the $n > 1$ case, this type of decline occurs and, as discussed earlier and in the work of *Whipple* [2001], the approximate analytical solution may

Table 3. Comparison of Analytical and Numerical Solutions for $n = 2$

L, km	$z_i(x_c)$, m	T_D Analytical, year	T_D Numerical, year[a]
10	1810	1.8×10^6	2.9×10^7
50	3350	3.3×10^6	5.3×10^7
100	4220	4.2×10^6	6.7×10^7

[a]Decay times calculated when erosion rate reached a minimum of 0.001 mm/yr.

Table 4. Comparison of Decay Times for Numerical and Analytical Solution for $n = 2/3$, 1, and 2[a]

	10% of Relief at x_c Left		1% of Relief at x_c Left		Minimum Erosion Rate of 0.001 mm/yr	
	T_D Analytical, Myr	T_D Numerical, Myr	T_D Analytical, Myr	T_D Numerical, Myr	T_D Analytical, Myr	T_D Numerical, Myr
$n = 2/3$	1.79	1.79	1.96	1.97	1.98	2.02
$n = 1$	1.79	1.79	1.96	2.01	1.98	2.25
$n = 2$	1.79	5.01	1.96	50.15	1.95	31.5

[a]Cut-off for decay time based on percent of relief left at channel head and erosion rate for 10 km channel.

significantly underestimate the decay time seen in numerical simulations (Tables 2 and 3).

5. Analysis

5.1. Model 1: One-Dimensional Detachment-Limited Numerical Simulations

[23] In order to explore the effects of numerical diffusion on model results and the behavior of the $n > 1$ case, a one-dimensional stream power erosion model was developed and tested against the analytical solution in equation (5). The code used for this model is a finite difference algorithm that solves equation (3) (with $\tau_c = 0$) over the domain $x_c < x < L$. In all simulations, a steady state profile (for the given values of U, K, L, and n) was used as the initial condition. At time $t = 0$ uplift is set to zero, all other parameters are held constant, and the channel erodes without any competition from uplift or isostatic rebound. The downstream end ($x = L$) is fixed at erosional baselevel. Response times for U, K, and L were determined to explore the dependence of these parameters on the decay timescale.

[24] Numerical solutions are generally accurate approximations of the analytical solutions provided that node spacing is sufficiently small so that numerical diffusion is not a significant problem. Since gradients are averaged over the discretization length scale, which acts to smear any abrupt changes in channel slope, node spacing must be small enough so that propagating knickpoints initiated at the downstream boundary by the change in boundary conditions (in this case a cessation of rock uplift rate) do not diffuse out, and cause a reduction of the channel gradient upstream of the knickpoint, thus substantially increasing the fluvial response time. The problem is naturally more severe for coarser grid spacings. Figure 3 shows examples of numerical diffusion for both $n \leq 1$ (Figures 3a and 3b) and $n > 1$ (Figure 3c). Figures 3a and 3b show the erosion rate at the channel head versus time for node spacings of 10 and 100 m for a 10-km channel. Numerical simulations were run in each case until the relief at the channel head reached 1% of the original relief. Also, shown is the analytical solution to the decay equation (vertical line). It can be seen that for coarse node spacing the numerical solution deviates from the analytical solution significantly, but for smaller node spacings the numerical solution closely approximates the analytical solution. In addition, Figure 3c demonstrates that for $n > 1$ deviation from the analytical solution is substantial even when models are run to 10% relief remaining ($\sim$2–3 times longer than analytical solution). The inset to Figure 3c shows that when the numerical model is run until only 1% relief remains, the decay time increases by a factor of $\sim$25. Even when models are run to minimum erosion rates of 0.001 mm/yr, decay times increase by a factor of 15–20. However, this is probably an unrealistic cutoff for the decay time since the final $\sim$10% of topography is erased over 80% of the total decay time (inset to Figure 3c). This becomes an important issue in the context of residual mountain ranges such as the Appalachians and Lachlan fold belt which arguably retain up to 25% of their initial, synorogenic relief [*Stephenson and Lambeck*, 1985; *Slingerland and Furlong*, 1989; *van der Beek and Braun*, 1999].

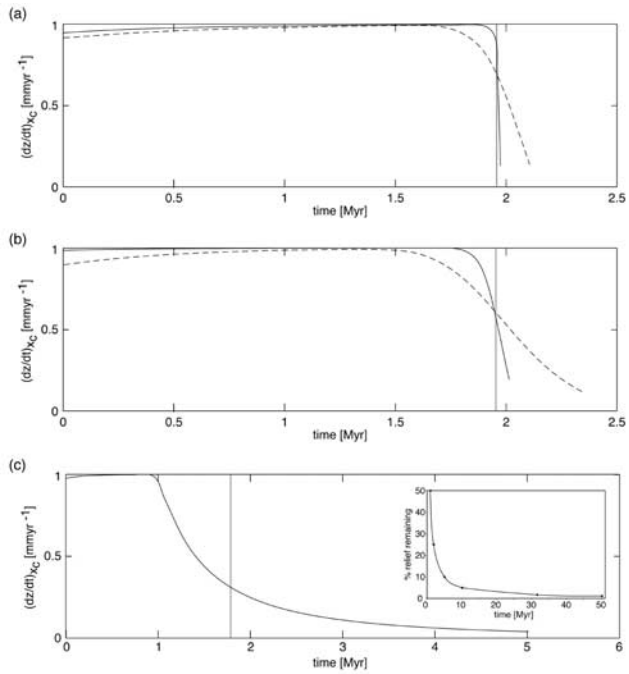

Figure 3. Comparison of numerical and analytical solutions for a 10-km channel for $n = 2/3$, 1, and 2 (a, b, and c, respectively). K was varied so that the initial relief was held constant for different values of n. Plots show how the erosion rate at the channel head evolves through time depending on the node spacing used. Dashed line indicates 100 m node spacing and solid black line indicates 10 m node spacing. The gray vertical line is the analytical solution. In Figures 3a and 3b, the numerical models were run until 1% of the initial relief at the channel head remained. For the $n = 2$ case, the plot shown in Figure 3c is the numerical model for 10 m node spacing run until 10% of the initial relief remained. The inset to Figure 3c shows the percent relief left at the channel head as a function of time, showing how the analytical solution for $n = 2$ severely underestimates the actual response time. See text for discussion.

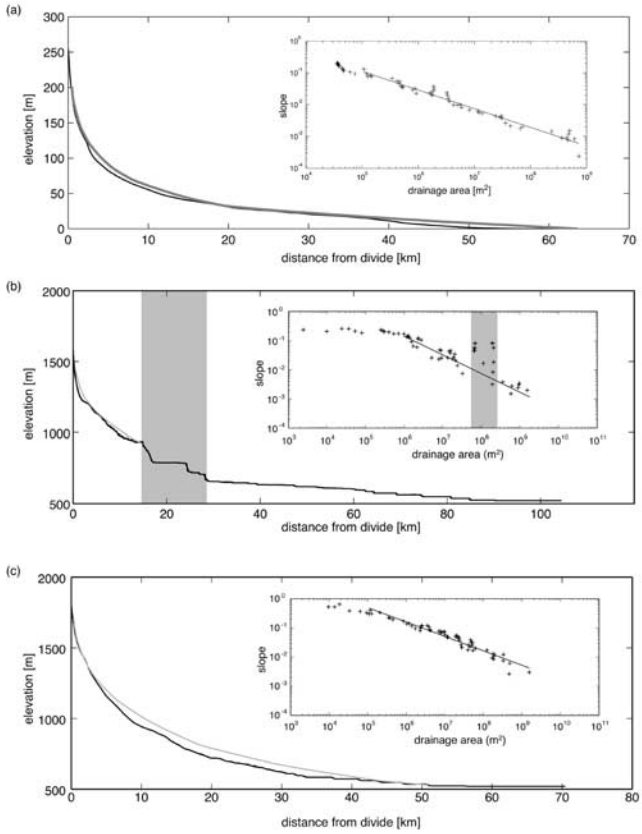

Figure 4. Longitudinal profiles from the Appalachians. Insets show plot of slope versus drainage area. (a) Middle River, Virginia in the Central Appalachians, (b) Tanasee Creek tributary of the Tuckasegee River, North Carolina Blue Ridge. The upper part drops over knickpoints where the stream crosses resistant quartz diorite and granodiorite (zone marked in gray). (c) East Fork of Raven Creek (a tributary to the Tuckasegee River). This river cuts mostly into metagraywacke, resulting in a smooth profile.

[25] As discussed earlier, for $n > 1$ a progressive decline in erosion rate of the channel head occurs and results in a marked increase in topographic decay time (Table 2). In addition, for $n > 1$ the channel profile evolves toward a characteristic declining form (time-invariant θ in equation (3) during decline), rather than the ''slope replacement'' style of profile evolution seen for $n < 1$ (see Figure 1). This characteristic form, as will be shown later, is very similar to the form of declining transport-limited channels [*Willgoose*, 1994].

[26] The main implications of the detachment-limited model for postorogenic decay times are that: (1) response times are very fast (2–5 Myr) for a reasonable range of model parameters (Table 3), (2) for $n \leq 1$ the topography decays in the ''slope replacement'' form, and (3) for $n > 1$ we see a ''declining'' decay form where slope reduction is more gradual and response times increase significantly, particularly for the removal of the final 10% of the original relief. Although very low values of the coefficient of erosion K predict very low-erosion rates, and thus very long topographic decay times, such low values of K imply unreasonably high initial steady state topographic relief. This strongly suggests that if there is a geomorphic explanation for the postorogenic persistence of mountainous topography, it must involve either isostatic uplift of a crustal root [e.g., *Stephenson*, 1984] or a progressive decline in the coefficient of erosion as the topography is reduced ($K = K(t)$) Moreover, the characteristic forms typical of residual topography (e.g., equation (3) is satisfied in the Appalachians (Figure 4)) [*Hack*, 1982] are only closely approximated by the detachment-limited model if $n > 1$. Sufficient topographic decay times are more realistically in the range of several hundreds of million years. Other explanations must therefore be entertained to account for a lengthening of the decay timescale. Possibilities include isostatic compensation, a transition to transport-limited conditions, and the effects of a critical shear stress and stochastic variability of flood magnitudes.

5.2. Model 2: Detachment-Limited Simulations With Isostatic Compensation

[27] Flexural isostasy was incorporated into the one-dimensional model in order to explore its effects on the decay timescale. The solution to the following fourth-order differential equation gives the amount of deflection along the channel:

$$D\frac{d^4w}{dx^4} + (\rho_m - \rho_c)gw = 0, \tag{8}$$

where ρ_c and ρ_m are the density of crust and mantle, respectively ($\rho_c = 2700$ kg/m^3 and $\rho_m = 3200$ kg/m^3), D is the flexural rigidity, g is the gravitational acceleration, and w is the vertical deflection [*Turcotte and Schubert*, 1982]. The flexural rigidity D depends on the elastic thickness of the crust H, as well as Young's modulus and Poisson's ratio.

[28] *Turcotte and Schubert* [1982] show that the flexural rigidity of the lithosphere can have a great effect on the degree of local isostatic compensation. The percentage of local isostatic compensation C that will be realized for periodic topography is a function of the density contrast between the crust and mantle, the flexural rigidity of the lithosphere, and the wavelength of the topography λ [*Turcotte and Schubert*, 1982, equation 3–117]:

$$C = \frac{(\rho_m - \rho_c)}{\rho_m - \rho_c + \dfrac{D}{g}\left(\dfrac{2\pi}{\lambda}\right)^4}. \tag{9}$$

[29] Solutions of equation (9) for a range of topographic wavelengths and elastic thicknesses are shown in Figure 5. This figure covers the width range of most orogenic belts in order to illustrate the range of conditions under which local isostatic compensation may be significant. It is apparent from this illustration that even a low-flexural rigidity is sufficient to suppress local compensation at topographic wavelengths less than about 100 km. Typical values for the elastic thickness of the crust are on the order of 10–30 km, so it is apparent that the intermediate-scale bedrock channels such as those considered in this analysis do not significantly deviate from nonisostatic runs for any effective elastic thickness >5 km (Figure 6). It is important to note that even the Swiss Alps and the Himalayas are only ~150 km wide, so that even for the longest bedrock channels, flexural isostatic compensation does not have a significant effect on decay timescales.

[30] In the extreme case, if complete isostatic compensation is achieved when the flexural rigidity is very small ($H = 0$) then the analysis shows that the decay time is

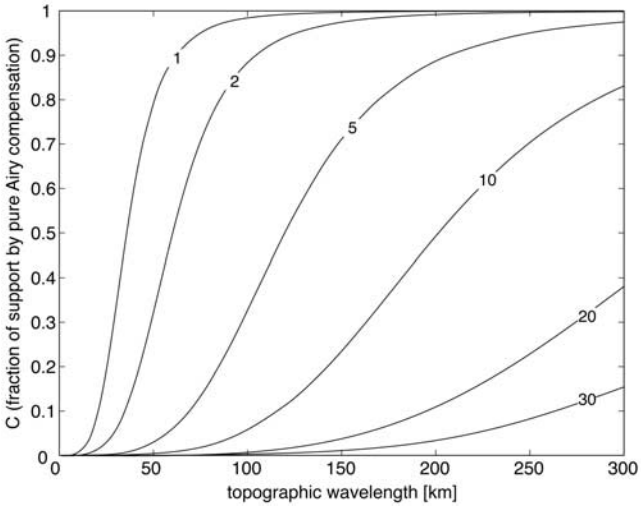

Figure 5. Degree of isostatic compensation for different elastic thicknesses (H). Elastic thicknesses for each line are shown by corresponding number in kilometers.

simply increased by a factor of 6 ($\rho_c/\rho_m - \rho_c) \approx 6$) for all values of the slope exponent n, and regardless of whether a detachment- or transport-limited model is used. Because of the density contrast between the crust and mantle, the amount of compensation achieved for a given timestep is approximately 5/6 of the amount of erosion. That is, for a given elevation dz of material eroded, the topography will respond isostatically by rebounding by 5/6 of this amount. Thus a conservative (maximum) estimate is that isostatic compensation leads to a factor of 6 increase in response time. Therefore for the $n \leq 1$ channels modeled in this study, decay times (for reducing to 1% of the original topography) are predicted to increase from 2–5 Myr to approximately 10–30 Myr. For the $n > 1$ case, the time it takes to reduce topography to 10% of the original lengthens from approximately 5 to 30 Myr. If we consider the case where topography is reduced to 1% of the original for the $n > 1$ case, then decay times lengthen to hundreds of million years since the remaining 10% of the topography is removed at extremely low-erosion rates. If we simply consider the case where 10% of the relief remains, then the decay times still severely underestimate realistic decay timescales in ancient orogens.

5.3. Model 3: Transport-Limited Erosion

[31] Transport-limited systems characteristically exhibit longer response times than detachment-limited systems, and evolve toward a characteristic form [*Willgoose*, 1994; *Whipple and Tucker*, 2002] similar to that observed in the Appalachians, the Lachlan fold belt, and the Urals [*Hack*, 1957, 1975, 1982; *Bishop et al.*, 1985; *Goldrick and Bishop*, 1995; *Bishop and Goldrick*, 2000] (Figure 4). Previous bedrock channel studies have shown that a transition from detachment- to transport-limited conditions is expected during decline [e.g., *Whipple and Tucker*, 2002]. Alluvial cover protects the channel bed, thus inhibiting erosion and potentially increasing decay times substantially [e.g., *Sklar and Dietrich*, 1998]. In order to examine the role of alluvial cover in more detail, two-dimensional modeling was used to explore both the purely transport-limited case as well as the transition from detachment- to transport-limited during postorogenic decline.

[32] Where long-term sediment input (Q_s) equals or exceeds long-term transport capacity (Q_c), the system is by definition transport-limited. For this case, the volumetric sediment flux, rather than erosion rate, is written as a power law function of unit stream power (or shear stress) [*Willgoose et al.*, 1991; *Tucker and Bras*, 1998]:

$$Q_c = K_t A^{m_t} S^{n_t}, \tag{10}$$

where K_t is a dimensional transport coefficient, and m_t and n_t are positive constants.

[33] A channel profile evolution equation based on equation (3) for a transport-limited system can be written as:

$$\frac{dz}{dt} = U - \frac{1}{1-\lambda_p}\frac{d}{dx}\frac{1}{W}(K_t A^{m_t} S^{n_t}), \tag{11}$$

where λ_p is the porosity of the sediment and W is the channel width.

[34] *Willgoose et al.* [1991] derived the expression for the relationship between steady state transport-limited channel gradients, where equation (11) becomes:

$$S_t = \left(\frac{\beta U}{K_t}\right)^{\frac{1}{n_t}} A^{-\theta_t}, \tag{12a}$$

$$\theta_t = (m_t - 1)/n_t, \tag{12b}$$

where θ_t is the intrinsic concavity of transport-limited systems, and is analogous to the detachment-limited case.

[35] *Whipple and Tucker* [2002] also present preliminary evidence that the intrinsic concavity indices of the detachment- and transport-limited systems are similar. Here we

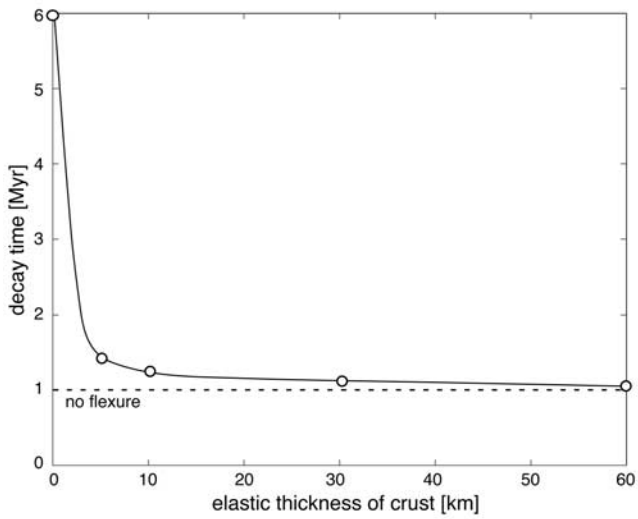

Figure 6. Dependence of decay timescale on elastic thickness for $n = 1$. Decay times for increasing elastic thicknesses quickly approach those of uncompensated simulations. For pure Airy isostasy, decay times are increased by a factor of 6 ($\rho_c/(\rho_c - \rho_m)$) compared to uncompensated simulations.

explore the simplest case where they are the same ($\theta_d = \theta_t$) An advantage of this case is that initial steady state topographies are identical for both the detachment- and transport-limited cases (compare equations (4) and (12) for $m/n = (m_t - 1)/n_t$); only the rate-limiting process varies in the simulations below. Under these conditions, *Whipple and Tucker* [2002] show that a sudden transition from detachment- to transport-limited is expected during postorogenic decline. This results in a partial protection of the bedrock channel floor from erosion [e.g., *Sklar and Dietrich*, 1998], a slowing of erosion, and, consequently, an increase in decay timescale.

[36] In order to evaluate the magnitude of the effect of a transition to transport-limited conditions on the decay timescale, we performed two-dimensional drainage basin evolution simulations with the landscape evolution model GOLEM [*Tucker and Slingerland*, 1994, 1996]. First, a steady state profile was generated by running the model until $dz/dt = 0$ everywhere along the channel. The first run was performed so that the initial condition is just at the threshold between detachment- and transport-limited (magnitude of fluvial coefficient of erosion K_t = magnitude of bedrock coefficient of erosion K_b). As shown in the work of *Whipple and Tucker* [2002], such systems will decline as predicted by the transport-limited model despite cutting through bedrock. Thus this case serves as the end-member transport-limited case. Then K_t was adjusted (set progressively larger than K_b), so that the initial condition is successively farther from the threshold condition. As K_t increases, the transition to transport-limited conditions will occur during decline, but not until more and more of the initial topography is erased. In the limit where $|K_t| \gg |K_b|$, model behavior converges on the pure detachment-limited case. This simple approach allows an approximate illustration of the influence of varying degrees of bed protection by a thin alluvial cover. More complex models may predict a stronger dependence between sediment flux and incision rate [e.g., *Sklar and Dietrich*, 1998; *Whipple and Tucker*, 2002], so these calculations are a conservative minimum estimate. Models were run until 1% of the mean elevation of the drainage basin remained. For the n =1 case, the pure detachment-limited case results in a decay time of 1.5 Myr, whereas the pure transport-limited case has a decay time of 4 Myr, increasing the response time by a factor of approximately 2–3. As K_t is set progressively larger than K_b, the system evolves to a longer period of detachment-limited erosion before the transition to transport-limited conditions takes place. Intermediate cases were run by increasing K_t such that the ratio of equilibrium slope for the detachment-limited system to the equilibrium slope for the transport-limited system increased from 1.5 to 3. This results in a gradual increase in response times for the transition from the end-member detachment-limited to the end-member transport-limited case. Figure 7 shows the results of these simulations by plotting the average elevation at the divide normalized to the initial steady state elevation at the divide as a function of time.

[37] In addition to increased response times, another interesting observation for the transport-limited case is the morphology of the topography as it decays. For a detachment-limited system, the topography is simply planed-off starting at the outlet and progressing back to the divide (Figure 8a). For transport-limited systems, however, the topography decays in a much more uniform manner, never completely erasing the topography at any given point. In this model, the slopes decrease gradually across the basin (Figure 8b). This form of decay is strikingly similar to the $n > 1$ case for a purely detachment-limited system. It is interesting to note that models which explain longer decay times (both transport- and detachment-limited for $n > 1$) share a characteristic form of slope decline [similar to that found in the work of *Willgoose*, 1994], consistent with observed topography in the Appalachians, Lachlan fold belt, and the Urals, as noted earlier (Figure 4) [*Hack*, 1957, 1975, 1982; *Bishop et al.*, 1985; *Goldrick and Bishop*, 1995; *Bishop and Goldrick*, 2000]. However, in each case, the modeling shows that the effects of alluvial cover are significant, but are nevertheless not dramatic enough to increase the decay timescale by a long enough time to account for the persistence of mountainous topography in ancient orogens, even when combined with pure Airy isostatic rebound of a thick crustal root. The resulting decay times for the $n \leq 1$ case combined with isostatic rebound predict maximum decay times of 36–90 Myr, depending on the length of the channel (10–100 km). For the $n > 1$ case, times are not substantially increased, since decay is already similar to that seen for systems in the transport-limited regime.

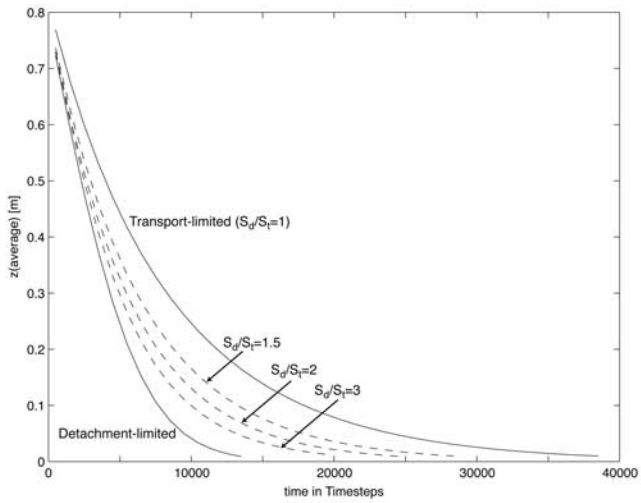

Figure 7. Transition from detachment-limited (DL) to transport-limited (TL) conditions for $n = 1$. Figure shows a plot of the average elevation of the channel head normalized to the initial elevation at the channel head through time. Simulations for the transition from DL to TL were set so that the initial condition is just at the threshold between DL and TL (fluvial coefficient of erosion K_t = bedrock coefficient of erosion K_b). This case serves as the limiting TL case. K_t was adjusted so that the initial condition is farther and farther from the purely transport-limited case ($S_d/S_t = 1.5$, $S_d/S_t = 2$, and $S_d/S_t = 3$ where S_d and S_t are the equilibrium slopes for the DL and TL systems, respectively).

5.4. Model 4: Critical Shear Stress and Stochastic Variability of Flood Discharge

[38] Analyses of landscape evolution using the stream power river incision model generally assume that any

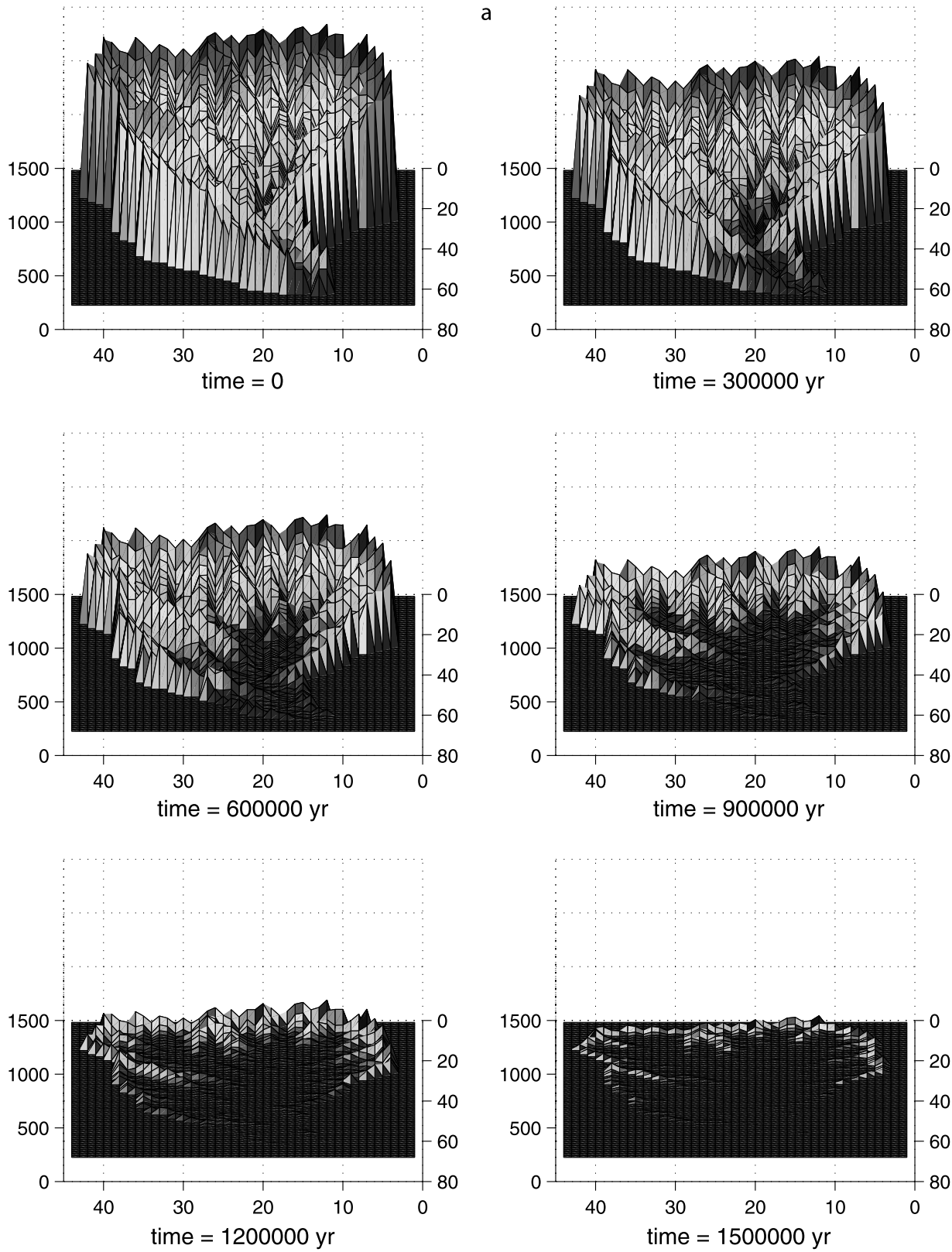

Figure 8. (a) Time slice examples of detachment-limited GOLEM simulations (elevation in m). Note the form of the decay is slope replacement and a flattening from the base upwards. Response time of system to reach 1% of the original mean drainage area relief is 1.5 Ma. (b) Time slice examples of transport-limited GOLEM simulations. Note the form of the decay is slope decline. A progressive decline in slope angles and stream gradients through time results in the production of a landsurface close to baselevel with very subdued relief. Response time of system to reach 1% of the original mean drainage area relief is 4 Ma.

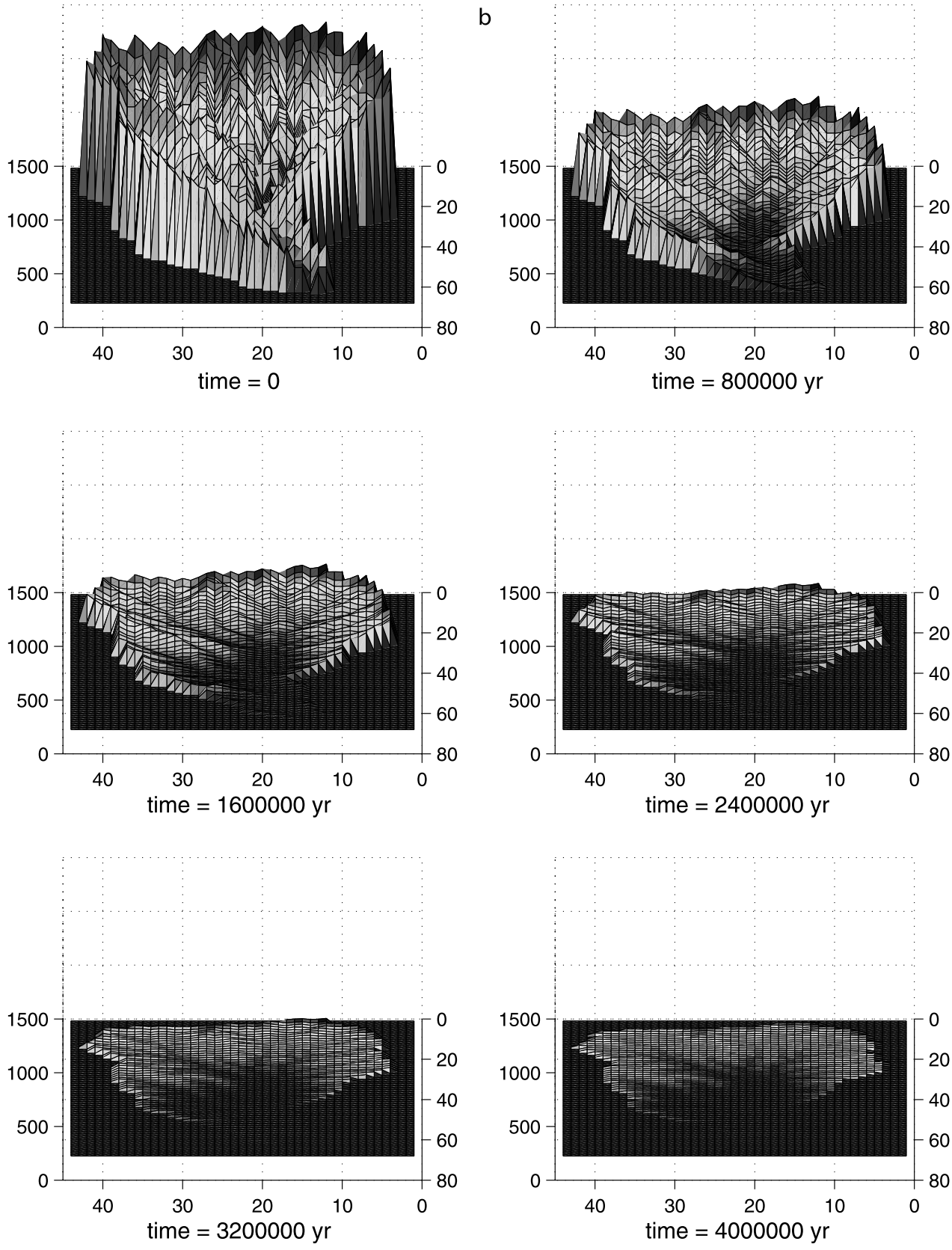

Figure 8. (continued)

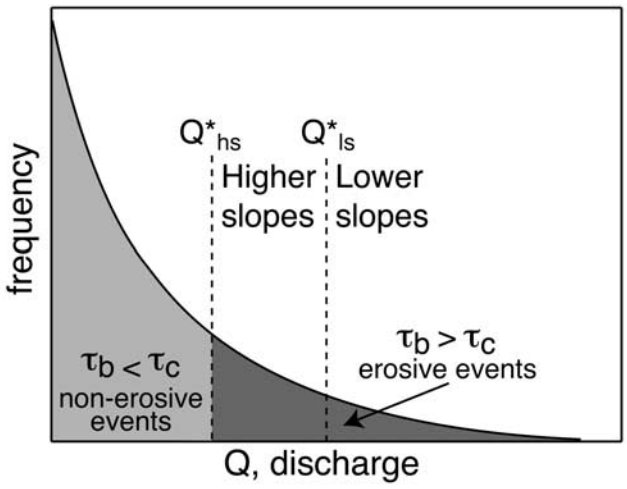

Figure 9. Plot of frequency of Q versus Q (discharge) showing the dependence of both slope and discharge on the likelihood of erosive events occurring. Q^*_{hs} is the critical discharge above which erosive events will take place for higher slopes and Q^*_{ls} is the critical discharge above which erosive events will take place for lower slopes. Erosive events will take place where the basal shear stress (τ_b) exceeds the critical shear stress for erosion (τ_c).

critical shear stress required for bedrock detachment is greatly exceeded by the floods of interest (i.e., that the coefficient of erosion K is set to an appropriate value to capture the magnitude and frequency of a ''geomorphically dominant'' discharge) such as the 5–10 year recurrence interval flood. However, including a critical shear stress for erosion can become quite important in the final stages of postorogenic topographic decay. For instance, the simple form of equation (2) predicts that erosion will proceed until shear stress (for the dominant flood) is everywhere reduced to the critical value. At this point, erosion ceases entirely. It can be shown analytically that the time to reach this final state of residual topography is roughly the same as for the $\tau_c = 0$ case described above (i.e., order of 1–10 Myr). However, in a sense this makes postorogenic topographic decay time infinite since there will always be significant residual topography, with residual relief set by the critical shear stress. Clearly, the ''dominant'' geomorphic discharge concept breaks down in this case. For any channel gradient, there will always be floods of some frequency and magnitude (Q^*) that produce shear stresses in excess of the erosion threshold. Importantly, however, as topography is reduced and stream gradients decline (unless there are compensating factors such as changes in hydraulic geometry, etc.), the frequency of geomorphically effective floods will decrease (i.e., Q^* increases to compensate for decreasing gradient, Figure 9). Therefore one may anticipate that the effective value of the coefficient of erosion (K_{eff}) will decline with time as channel gradients are reduced, potentially increasing the topographic decay timescale significantly.

[39] We use the stochastic-storm-driven detachment-limited model of *Tucker and Bras* [2000] to illustrate the combined effect of a critical shear stress for erosion and a stochastic distribution of flood magnitudes. As *Tucker and Bras* [2000] point out, the ''standard'' form of their model (equivalent of equation (2a)) can only be solved numerically. However, if a model with the form of equation (2b) is adopted, an analytical solution for K_{eff} as a function of channel gradient is more tractable and has been described by *Tucker* [2003]. We use this form for convenience, while noting that results will differ in detail from those obtained using the standard form of equation (2a) in numerical simulations. A simplified representation of the *Tucker and Bras* [2000] model can be written as:

$$E = K_{\text{eff}} A^m S^n, \tag{13}$$

$$K_{\text{eff}} = K_r K_c \beta_{\tau c}, \tag{14}$$

where K_r describes the substrate resistance to erosion and the efficiency of the erosion process, K_c describes the climate (including mean annual precipitation and storminess), and $\beta_{\tau c}$ is a term that describes the fraction of the frequency distribution of floods that contribute to erosion of the bed (as illustrated in cartoon fashion in Figure 9). The fraction $\beta_{\tau c}$ varies from 0 to 1 as a function of channel gradient and the critical shear stress. For $\tau_c = 0$, $\beta_{\tau c}$ takes a value of unity (all floods contribute to erosion). As τ_c increases or channel gradient decreases, $\beta_{\tau c}$ asymptotically approaches zero (Figure 10).

[40] Parameters used for numerical simulations are shown in Table 5. Modern climate parameters for Georgia were used following the work of *Tucker and Bras* [2000]. Simulations were run from steady state topography for a 10-km channel with 3155 m of initial relief. The decay time for the $n = 1$ case was 37 Myr, compared to 2 Myr for the analytical solution to the detachment-limited case, increasing response time by almost a factor of 20. The final state of the stochastic case was chosen when erosion rates fell to 0.001 mm/yr. At this point, however, 8% of the original

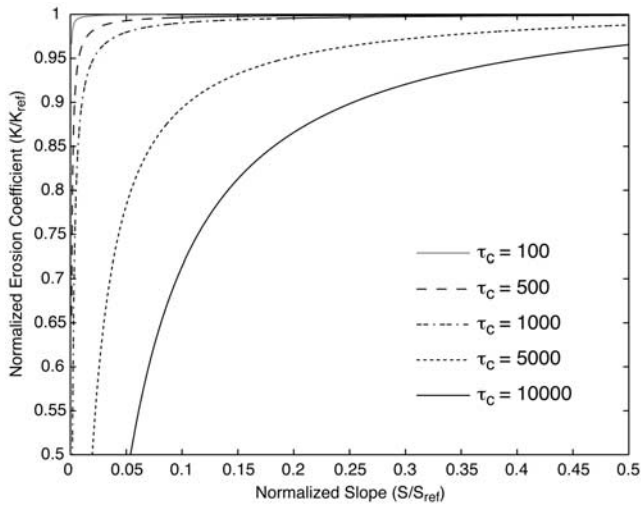

Figure 10. Plot of K_{eff} declining with decreasing slope for different values of τ_c.

Table 5. Parameter Values Used in Critical Shear Stress and Stochastic Variability of Flood Discharge Numerical Simulations[a]

Parameter	Value
Average rainfall rate ($\bar{P}$)	16.4 m/yr
Duration (T_r)	7.9 years
Interstorm interval duration ($\bar{T}_b$)	100 years
Infiltration capacity (I)	0 mm/h
Erosion efficiency constant (k_e)	1×10^{-5} m/yr^1
Channel width-discharge coefficient (k_t)	1.4×10^3 kg/m$^{2.2}$/s$^{1.4}$
Discharge coefficient (k_w)	12.7 m$^{1/2}$/s$^{1/2}$
Critical runoff intensity (R_c)	1×10^{-7}m/yr
Critical shear stress (τ_c)	114 N/m^2
Width-discharge exponent (α)	2/3
Slope exponent (β)	0.7
Shear stress exponent (a)	3/2
At-a-station channel width exponent (ω_s)	0.25
Downstream channel-width exponent (ω_b)	0.5

[a]From *Tucker and Bras* [2000].

topography remained (240 m) (Figure 11a). Of course, both the decay timescale and the height of residual topography depend on climate and the magnitude of τ_c. This example simulation, however, serves to show that: (1) decay times may be substantially increased by including a minimal realistic critical shear stress [*Snyder*, 2001], and perhaps more importantly, (2) a significant portion of topography remains by the time these low erosion rates are reached. Therefore a critical shear stress for erosion may be a key parameter to include in accounting for the persistence of relict topography. That is, by the time weathering takes over as the rate-limiting process there still might be hundreds of meters of topography remaining, which may require up to several hundred million years of additional time to reduce by weathering-limited processes.

6. Discussion and Conclusions

[41] The survival of postorogenic topography for hundreds of millions of years is a long-standing problem in geomorphology and geodynamics. Viable models to explain the persistence of topography in ancient orogenic belts must not only explain this timescale of the decay (on the order of hundreds of million years), but also explain the morphology, or characteristic form, of the residual topography. For a pure detachment-limited system (Model 1) with $n \leq 1$ the response times are very fast (typically 1–10 Myr). However, if $n > 1$ the approximate analytical solution can be expected to significantly underestimate response time, resulting in decay times that are substantially longer. For example, these times still significantly underestimate the age of the existing topography we see at the present day in the Central Appalachians. Therefore we have explored a variety of processes that act to inhibit erosion, resulting in increased decay times. Incorporating Airy isostatic rebound of a thick orogenic root (Model 2) simply increases the decay time by a factor of 6, which is still insufficient to explain the persistence of relict mountainous topography for $n \leq 1$ (10–30 Myr). For models with $n > 1$ still only results in increasing decay times to a few tens of million years. Decay times of several hundred million years can only be achieved for the $n > 1$ case after the removal of the final 10% of the topography, during which erosion rates are less than 0.001 mm/yr. However, this case is only achieved for very weak crust. Adding flexural strength greatly reduces the isostatic compensation for the topographic wavelengths investigated (10–100 km).

[42] In all detachment-limited simulations with $n \leq 1$ channels decay in the slope replacement form, with river profiles simply being planed-off from the outlet to the divide (e.g., see Figures 1 and 8a). However, in models with $n > 1$ channels decay in a characteristic form of slope decline similar to that described by *Willgoose* [1994] for transport-limited conditions, reproducing the characteristic form of residual topography of the Central Appalachians, for example (Figures 4 and 8b).

[43] The analysis of detachment-limited bedrock channels clearly shows that unless $n > 1$, either there are serious deficiencies in the detachment-limited model or that postorogenic nonisostatic uplift has occurred. For this reason, the transition to transport-limited conditions during postorogenic decline predicted by *Whipple and Tucker* [2002] was considered in order to evaluate its effect on the decay timescale.

[44] Landscape evolution models that track both the detachment-limited erosion and the transport of sediment delivered to the channels predict a transition to transport-limited conditions during postorogenic decline (Model 3).

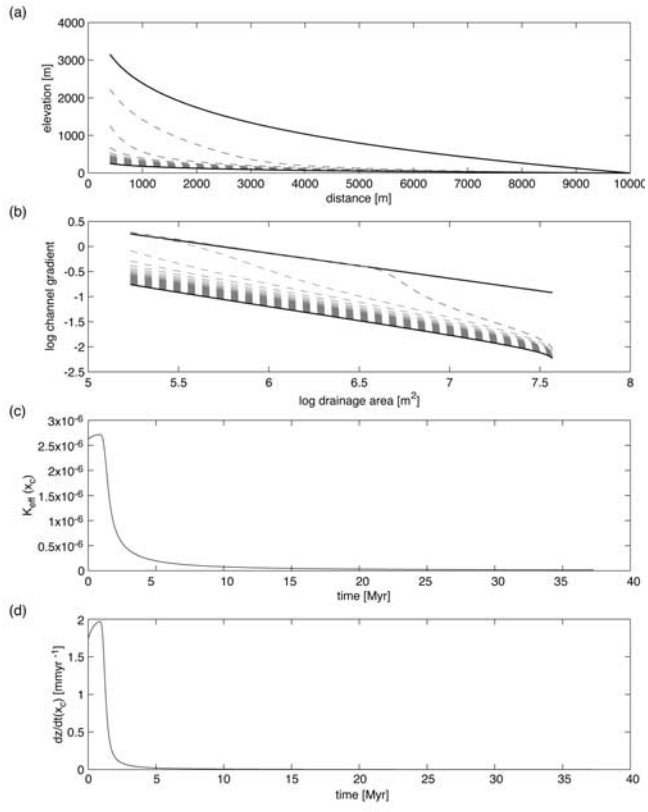

Figure 11. Example of stochastic numerical simulation for $n = 1$. (a) Longitudinal profile with transient curves. Note characteristic form of decay becomes similar to that expected for transport-limited conditions as topography is reduced. (b) Slope-area relationship. (c) K_{eff} at the channel head through time. (d) Erosion rate at the channel head through time.

The transition to transport-limited conditions involves a partial protection of the channel bed from erosion by a thin alluvial cover and a commensurate decrease in erosion rate. Incorporating this transition into the model increases response times by at most a factor of 2–3 (36–90 Myr if full isostatic rebound occurs), but, more importantly, the morphology of the decay takes on a characteristic slope decline form, similar to the $n > 1$ case for detachment-limited conditions. Although this transition to transport-limited conditions is clearly important, these decay times are still insufficient to explain the persistence of residual mountainous topography. The final layer of complexity considered in this study was the incorporation of the combined effects of a critical threshold for erosion and the stochastic variability of flood magnitudes. Including a critical shear stress (Model 4) is likely to be important since as topography decays only the larger magnitude, less frequent storms will exceed this critical shear stress, resulting in a progressive reduction in the effective coefficient of erosion, greatly enhancing decay times. While this increases decay times by approximately a factor of 20 (depending on the value of τ_c and the frequency of large floods), more importantly, weathering rate probably becomes limiting while significant postorogenic topography remains (up to hundreds of meters) for minimal realistic values of τ_c. We feel this provides a viable explanation for the survival of such subdued topography in ancient orogenic belts. In addition, this model reproduces the characteristic slope decline form of residual channels (Figure 11). Thus a model incorporating isostasy, critical shear stress and stochastic distribution of storms, and either $n > 1$ or a transition from detachment- to transport-limited conditions may explain long decay times without appealing to postorogenic uplift. Further field studies of critical shear stress and stochastic storms are needed to constrain model parameters in a range of geologic conditions to fully evaluate the importance of their influence.

Notation

n slope exponent, erosion rule,
n_t slope exponent, bed load transport rule,
m area exponent, detachment-limited erosion rule,
m_t area exponent, bed load transport rule,
t time, T,
w vertical deflection, L,
z elevation of streambed, L,
A upstream drainage area, L^2,
C degree of compensation,
D flexural rigidity [N m],
E vertical erosion rate, L/T,
H elastic thickness of crust, L,
K coefficient of erosion, L^{1-2m}/T,
K_t bed load transport coefficient, L^{3-2mt}/T,
L channel length scale, L,
Q_c bed load sediment transport capacity, L^3/T,
Q_s bed load sediment flux, L^3/T,
S streamwise channel bed gradient,
S_d steady state gradient of detachment-limited streams,
S_t steady state gradient of transport-limited streams,
T_D topographic decay time, T,
U rock uplift rate, L/T,
U_{cr} critical rock uplift rate for a transition from detachment- to transport-limited conditions, L/T,
W channel width, L,
β fraction of sediment delivered to channels as bed load,
λ wavelength, L,
λ_p bed sediment porosity,
θ stream concavity index (scaling exponent in gradient-area relationship),
θ_d intrinsic concavity index of detachment-limited systems,
θ_t intrinsic concavity index of transport-limited systems,
ρ_m density of crust [kg/m^3],
ρ_c density of mantle [kg/m^3],
τ_b basal shear stress,
τ_c critical shear stress.

[45] **Acknowledgments.** We thank P. Molnar for pointing out the second form of the steam power model (equation (1b)). Critical reviews by R. Anderson and an anonymous reviewer greatly improved the original manuscript. An earlier version of this paper benefited from reviews by S. Brocklehurst, E. Kirby, and N. Snyder.

References

Berzin, R., O. Oncken, J. H. Knapp, A. Perez-Estaun, T. Hismatulin, N. Yunusov, and A. Lipilin, Orogenic evolution of the Ural Mountains; results from an integrated seismic experiment, *Science*, *274*, 220–221, 1996.

Bierman, P., and J. Turner, 10Be and 26Al evidence for exceptionally low rates of Australian bedrock erosion and the likely existence of pre-Pleistocene landscapes, *Quat. Res.*, *44*, 378–382, 1995.

Bishop, P., and G. Goldrick, Geomorphological evolution of the East Australian continental margin, in *Geomorphology and Global Tectonics*, edited by M. A. Summerfield, pp. 225–254, John Wiley, New York, 2000.

Bishop, P., R. W. Young, and I. McDougall, Stream profile change and longterm landscape evolution: Early miocene and modern rivers of the East Australian Highland Crest, central New South Wales, Australia, *J. Geol.*, *93*, 455–474, 1985.

Brown, R. W., M. A. Summerfield, and A. J. W. Gleadow, Apatite fission track analysis: Its potential for the estimation of denudation rates and implications for models of long-term landscape development, in *Process Models and Theoretical Geomorphology*, edited by M. J. Kirkby, pp. 24–53, John Wiley, New York, 1994.

Browne, W. R., The geology of New South Wales, *J. Geol. Soc. Aust.*, *16*, 559–569, 1969.

Carbonell, R., A. Perez-Estaun, J. Gallart, J. Diaz, S. Kashubin, J. Mechie, R. Stadtlander, A. Schulze, J. H. Knapp, and A. Morozov, Crustal root beneath the Urals: Wide-angle seismic evidence, *Science*, *274*, 222–224, 1996.

Costain, J. K., R. D. Hatcher Jr., C. Coruh, T. L. Pratt, S. R. Taylor, J. J. Litehiser, and I. Zietz, Geophysical characteristics of the Appalachian crust, in *The Appalachian-Ouachita Orogen in the United States*, *Geol North Am.*, vol. F-2, edited by R. D. Hatcher Jr., W. A. Thomas, and G. W. Viele, pp. 385–416, Geol. Soc. of Am., Boulder, Colo., 1989.

Davis, W. M., The rivers and valleys of Pennsylvania, *Nat. Geog. Mag.*, *1*, 183–253, 1889.

Davis, W. M., The Basin Range problem, *Proc. Natl. Acad. Sci. U. S. A.*, *11*(7), 387–392, 1925.

Fairbridge, R. W., and C. W. Finkl Jr., Cratonic erosional unconformities and peneplains, *J. Geol.*, *88*, 69–86, 1980.

Fernandes, N. F., and W. E. Dietrich, Hillslope evolution by diffusive processes: The timescale for equilibrium adjustments, *Water Resour. Res.*, *33*(6), 1307–1318, 1997.

Flint, J. J., Stream gradient as a function of order, magnitude, and discharge, *Water Resour. Res.*, *10*, 969–973, 1974.

Foley, M. G., Bed-rock incision by streams, *Geol. Soc. Am. Bull.*, *91*, 2189–2213, 1980.

Gilluly, J., Geologic contrasts between continents and ocean basins, *Geol. Soc. Am. Spec. Publ.*, *52*, 7–18, 1955.

Goldrick, G., and P. Bishop, Differentiating the roles of lithology and uplift in the steepening of bedrock river long profiles: An example from southeastern Australia, *J. Geol.*, *103*, 227–231, 1995.

Gray, D. R., Tectonics of the southeastern Australian Lachlan fold belt; structural and thermal aspects, in *Orogeny Through Time*, edited by J.-P. Burg and M. Ford, *Geol. Soc. Spec. Publ.*, 149–177, 1997.

Hack, J. T., Studies of longitudinal stream profiles in Virginia and Maryland, *U. S. Geol. Surv. Prof. Pap.*, *294-B*, 42–97, 1957.

Hack, J. T., Interpretation of erosional topography in humid temperate regions, in *Planation Surfaces: Peneplains, Pediplains, and Etchplains*, *Benchmark Pap. Geol.*, vol. 22, edited by G. F. Adams, pp. 129–146, Dowden, Hutchinson and Ross, Stroudsburg, Pa., 1975.

Hack, J. T., Physiographic divisions and differential uplift in the Piedmont and Blue Ridge, *U. S. Geol. Surv. Prof. Pap.*, *1265-P*, 1–49, 1982.

Hancock, G. S., R. S. Anderson, and K. X. Whipple, Beyond power: Bedrock river incision processes and form, in *Rivers Over Rock: Fluvial Processes in Bedrock Channels*, edited by K. J. Tinkler and E. E. Wohl, pp. 35–60, AGU, Washington, D. C., 1998.

Heimsath, A. M., W. E. Dietrich, K. Nishiizumi, and R. C. Finkel, The soil production function and landscape equilibrium, *Nature*, *388*, 358–361, 1997.

Howard, A. D., A detachment-limited model of drainage basin evolution, *Water Resour. Res.*, *30*(7), 2261–2285, 1994.

Howard, A. D., and G. Kerby, Channel changes in badlands, *Geol. Soc. Am. Bull.*, *94*, 739–752, 1983.

Howard, A. D., W. E. Dietrich, and M. A. Seidl, Modeling fluvial erosion on regional to continental scales, *J. Geophys. Res.*, *99*(B7), 13,971–13,986, 1994.

Jacobs, J. A., R. D. Russell, and J. T. Wilson, *Physics and Geology*, p. 424, 1959.

Judson, S., Evolution of Appalachian topography, in *Theories of Landform Development*, *Binghamton Symp. Geomorphol.: Int. Ser.*, vol. 6, edited by W. N. Melhorn and R. C. Flemal, pp. 29–44, State Univ. of N. Y., Binghamton, 1975.

Judson, S., and D. F. Ritter, Rates of regional denudation in the United States, *J. Geophys. Res.*, *69*(16), 3395–3401, 1964.

Kirby, E., and K. Whipple, Quantifying differential rock-uplift rates via stream profile analysis, *Geology*, *29*, 415–418, 2001.

Kruse, S. E., and M. McNutt, Compensation of Paleozoic orogens; a comparison of the Urals to the Appalachians, *Tectonophysics*, *154*(1–2), 1–17, 1988.

Lambeck, K., and R. Stephenson, Post-orogenic evolution of a mountain range; south-eastern Australian highlands, *Geophys. Res. Lett.*, *12*, 801–804, 1985.

Lister, G. A., and M. A. Etheridge, Detachment models for uplift and volcanism in the eastern highlands, and their application to the origin of passive margin mountains, in *Intraplate Volcanism in Eastern Australia and New Zealand*, edited by R. W. Johnson, pp. 297–313, Cambridge Univ. Press/Aust. Acad. of Sci., New York, 1989.

Melhorn, W. N., and D. E. Edgar, The case for episodic, continental scale erosion surfaces: A tentative geodynamic model, in *Theories of Landform Development*, edited by W. N. Melhorn and R. C. Flemal, pp. 243–272, Binghamton State Univ. of N. Y., Binghamton, 1975.

Meyerhoff, H. A., Postorogenic development of the Appalachians, *Geol. Soc. Am. Bull.*, *83*(6), 1709–1727, 1972.

Moglen, G. E., and R. L. Bras, The effect of spatial heterogeneities on geomorphic expression in a model of basin evolution, *Water Resour. Res.*, *31*(10), 2613–2623, 1995.

Ollier, C. D., Tectonics and geomorphology of the eastern highlands, in *Landform Evolution in Australia*, edited by J. L. Davies and M. A. J. Williams, pp. 5–47, Aust. Natl. Univ. Press, Canberra, 1978.

Ollier, C. D., The Great Escarpment of eastern Australia; tectonic and geomorphic significance, *J. Geol. Soc. Aust.*, *29*(1–2), 13–23, 1982.

Ollier, C. D., Morphotectonics of passive continental margins, *Z. Geomorphol. Suppl.*, *54*, 120 pp., 1985.

Ollier, C. D., and C. F. Pain, Landscape evolution and tectonics in southeastern Australia, *AGSO J. Aust. Geol. Geophys.*, *15*, 335–345, 1994.

Ollier, C. D., and C. F. Pain, Reply: Landscape evolution and tectonics in southeastern Australia (Ollier and Pain 1994), *AGSO J. Aust. Geol. Geophys.*, *16*, 325–331, 1996.

Pazzaglia, F. J., and M. T. Brandon, Macrogeomorphic evolution of the post-Triassic Appalachian mountains determined by deconvolution of the offshore basin sedimentary record, *Basin Res.*, *8*, 255–278, 1996.

Pazzaglia, F. J., and T. W. Gardner, Late Cenozoic flexural deformation of the middle U. S. Atlantic passive margin, *J. Geophys. Res.*, *99*(B6), 12,143–12,157, 1994.

Pazzaglia, F. J., T. W. Gardner, and D. J. Merritts, Bedrock fluvial incision and longitudinal profile development over geologic time scales determined by fluvial terraces, in *Rivers Over Rock: Fluvial Processes in Bedrock Channels*, edited by K. J. Tinkler and E. E. Wohl, pp. 207–236, AGU, Washington, D. C., 1998.

Pinet, P., and M. Souriau, Continental erosion and large-scale relief, *Tectonics*, *7*(3), 563–582, 1988.

Poag, C. W., W. D. Sevon, and T. W. Gardner, A record of Appalachian denudation in postrift Mesozoic and Cenozoic sedimentary deposits of the U. S. Middle Atlantic continental margin, *Geomorphology*, *2*, 119–157, 1989.

Rosenbloom, N. A., and R. S. Anderson, Evolution of the marine terraced landscape, Santa Cruz, California, *J. Geophys. Res.*, *99*, 14,013–14,030, 1994.

Royden, L. H., M. K. Clark, and K. X. Whipple, Evolution of river elevation profiles by bedrock incision: Analytical solutions for transient river profiles related to changing uplift and precipitation rates, *Eos Trans. AGU*, *81*(48), Fall Meet. Suppl., F1142, 2000.

Schumm, S. A., The disparity between present rates of denudation and orogeny, *U. S. Geol. Surv. Prof. Pap.*, *454-H*, 1–13, 1963.

Schumm, S. A., and R. W. Lichty, Time, space, and causality in geomorphology, *Am. J. Sci.*, *263*(2), 110–119, 1965.

Seidl, M. A., and W. E. Dietrich, The problem of channel erosion into bedrock, *Catena Suppl.*, *23*, 101–124, 1992.

Sinclair, K., and R. C. Ball, Mechanism for global optimization of river networks from local erosion rules, *Phys. Rev. Lett.*, *76*(18), 3360–3363, 1996.

Sklar, L., and W. E. Dietrich, River longitudinal profiles and bedrock incision models: Stream power and the influence of sediment supply, in *Rivers Over Rock: Fluvial Processes in Bedrock Channels*, edited by K. J. Tinkler and E. E. Wohl, pp. 237–260, AGU, Washington, D. C., 1998.

Slingerland, R., Systematic slope-area functions in the Central Range of Taiwan may imply topographic unsteadiness, *Geol. Soc. Am. Abstr. Programs*, *31*, 296, 1999.

Slingerland, R., and K. P. Furlong, Geodynamic and geomorphic evolution of the Permo-Triassic Appalachian Mountains, *Geomorphology*, *2*, 23–37, 1989.

Slingerland, R., S. D. Willett, and N. Hovius, Slope-area scaling as a test of fluvial bedrock erosion laws, *Eos Trans. AGU*, *79*(45), Fall Meet. Suppl., F358, 1998.

Small, E. E., R. S. Anderson, J. L. Repka, and R. Finkel, Erosion rates of alpine bedrock summit surfaces deduced from in situ 10Be and 26Al, *Earth Planet. Sci. Lett.*, *150*, 413–425, 1997.

Small, E. E., R. S. Anderson, and G. S. Hancock, Estimates of the rate of regolith production using 10Be and 26Al from an alpine hillslope, *Geomorphology*, *27*, 131–150, 1999.

Snyder, N. P., Bedrock channel response to tectonic, climatic, and eustatic forcings, Ph.D. thesis, 142 pp., Mass. Inst. of Technol., Cambridge, 2001.

Snyder, N. P., K. X. Whipple, G. E. Tucker, and D. J. Merritts, Landscape response to tectonic forcing: Digital elevation model analysis of stream profiles in the Mendocino triple junction region, northern California, *GSA Bull.*, *112*, 1250–1263, 2000.

Stephenson, R., Flexural models of continental lithosphere based on long-term erosional decay of topography, *Geophys. J. R. Astron. Soc.*, *77*, 385–413, 1984.

Stephenson, R., and K. Lambeck, Erosion-isostatic rebound models for uplift: An application to south-eastern Australia, *Geophys. J. R. Astron. Soc.*, *82*, 31–55, 1985.

Stock, J. D., and D. R. Montgomery, Geologic constraints on bedrock river incision using the stream power law, *J. Geophys. Res.*, *104*(B3), 4983–4993, 1999.

Tarboton, D. G., R. L. Bras, and I. Rodriguez-Iturbe, Scaling and elevation in river networks, *Water Resour. Res.*, *25*(9), 2037–2051, 1989.

Tarboton, D. G., R. L. Bras, and I. Rodriguez-Iturbe, On the extraction of channel networks from digital elevation data, *Hydrol. Process.*, *5*, 81–100, 1991.

Thornbury, W. D., *Principles of Geomorphology*, 618 pp., John Wiley, New York, 1962.

Tinkler, K., and E. E. Wohl, *Rivers Over Rock: Fluvial Processes in Bedrock Channels*, 323 pp., AGU, Washington, D. C., 1998.

Tucker, G. E., Drainage basin sensitivity to tectonic and climatic forcing: Implications of a stochastic model for the role of entrainment and erosion thresholds, *Earth Surf. Processes Landforms*, in press, 2003.

Tucker, G. E., and R. L. Bras, Hillslope processes, drainage density, and landscape morphology, *Water Resour. Res.*, *34*, 2751–2764, 1998.

Tucker, G. E., and R. L. Bras, A stochastic approach to modeling the role of rainfall variability in drainage basin evolution, *Water Resour. Res.*, *36*(7), 1953–1964, 2000.

Tucker, G. E., and R. L. Slingerland, Erosional dynamics, flexural isostasy, and long-lived escarpments: A numerical modeling study, *J. Geophys. Res.*, *99*(B6), 12,229–12,243, 1994.

Tucker, G. E., and R. L. Slingerland, Predicting sediment flux from fold and thrust belts, *Basin Res.*, *8*, 329–349, 1996.

Tucker, G. E., and K. X. Whipple, Topographic outcomes predicted by stream erosion models: Sensitivity analysis and intermodel comparison, *J. Geophys. Res.*, *107*(B9), 2179, doi:10.1029/2001JB000162, 2002.

Turcotte, D. L., and G. Schubert, *Geodynamics: Applications of Continuum Mechanics to Geological Problems*, 450 pp., John Wiley, New York, 1982.

Twidale, C. R., On the survival of paleoforms, *Am. J. Sci.*, *276*(1), 77–95, 1976.

van der Beek, P., and J. Braun, Controls on post-mid-Cretaceous landscape evolution in the southeastern highlands of Australia: Insights from numerical surface process models, *J. Geophys. Res.*, *104*(B3), 4945–4966, 1999.

Weissel, J. K., and M. A. Seidl, Inland propagation of erosional escarpments and river profile evolution across the southeastern Australian passive continental margin, in *Rivers Over Rock: Fluvial Processes in Bedrock Channels*, edited by K. Tinkler and E. E. Wohl, pp. 189–206, AGU, Washington, D. C., 1998.

Wellman, P., On the isostatic compensation of Australian topography, *BMR J. Aust. Geol. Geophys.*, *4*(4), 373–382, 1979.

Whipple, K. X., Fluvial landscape response time: How plausible is steady-state denudation?, *Am. J. Sci.*, *301*, 313–325, 2001.

Whipple, K. X., and G. E. Tucker, Dynamics of the stream-power river incision model: Implications for height limits of mountain ranges, landscape response timescales, and research needs, *J. Geophys. Res.*, *104*, 17,661–17,674, 1999.

Whipple, K. X., and G. E. Tucker, Implications of sediment-flux-dependent river incision models for landscape evolution, *J. Geophys. Res.*, *107*(B2), 2039, doi:10.1029/2000JB000044, 2002.

Whipple, K. X., G. S. Hancock, and R. S. Anderson, River incision into bedrock: Mechanics and relative efficacy of plucking, abrasion, and cavitation, *GSA Bull.*, *112*(3), 490–503, 2000.

Willgoose, G., A physical explanation for an observed area-slope-elevation relationship for catchments with declining relief, *Water Resour. Res.*, *30*(2), 151–159, 1994.

Willgoose, G., R. L. Bras, and I. Rodriguez-Iturbe, A coupled channel network growth and hillslope evolution model, *Water Resour. Res.*, *27*(7), 1671–1684, 1991.

Wohl, E. E., Bedrock channel morphology in relation to erosional processes, in *Rivers Over Rock: Fluvial Processes in Bedrock Channels*, edited by K. J. Tinkler and E. E. Wohl, pp. 133–151, AGU, Washington, D. C., 1998.

Wohl, E. E., N. Greenbaum, A. P. Schick, and V. R. Baker, Controls on bedrock channel incision along Nahal Paran, Israel, *Earth Surf. Processes Landforms*, *19*, 1–13, 1994.

Young, R. W., Crustal constraints on the evolution of the continental divide of eastern Australia, *Geology*, *17*(6), 528–530, 1989.

Young, R., and I. McDougall, Long-term landscape evolution: Early Miocene and Modern Rivers in southern New South Wales, Australia, *J. Geol.*, *101*, 35–49, 1993.

J. A. Baldwin and K. X. Whipple, Department of Earth, Atmospheric, and Planetary Sciences, Massachusetts Institute of Technology, Cambridge, MA 02139, USA. (jbaldwin@mit.edu)

G. E. Tucker, School of Geography and the Environment, University of Oxford, Oxford, OX1 3TB, UK.